Placenta 139 (2023) 34–42

Contents lists available at ScienceDirect

Placenta

journal homepage: www.elsevier.com/locate/placenta

Identification of a unique intervillous cellular signature in chronic histiocytic intervillositis

Juliette Krop [a], Lotte E. van der Meeren [b,c], Marie-Louise P. van der Hoorn [d], Marieke E. Ijsselsteijn [b], Kyra L. Dijkstra [b], H. Kapsenberg [a], C. van der Keur [a], Emily F. Cornish [e], Peter G.J. Nikkels [f], Frits Koning [a], Frans H.J. Claas [a], Sebastiaan Heidt [a], Michael Eikmans [a,*,1], Manon Bos [b,d,1]

[a] Department of Immunology, Leiden University Medical Centre, Leiden, the Netherlands
[b] Department of Pathology, Leiden University Medical Centre, Leiden, the Netherlands
[c] Department of Pathology, Erasmus Medical Center, Rotterdam, the Netherlands
[d] Department of Gynecology and Obstetrics, Leiden University Medical Centre, Leiden, the Netherlands
[e] Elizabeth Garrett Anderson Institute for Women's Health, University College London, London, UK
[f] Department of Pathology, University Medical Center Utrecht, Utrecht, the Netherlands

A B S T R A C T

Introduction: Chronic histiocytic intervillositis (CHI) is a rare histopathological lesion in the placenta characterized by an infiltrate of $CD68^+$ cells in the intervillous space. CHI is associated with adverse pregnancy outcomes such as miscarriage, fetal growth restriction, and (late) intrauterine fetal death. The adverse pregnancy outcomes and a variable recurrence rate of 25–100% underline its clinical relevance. The pathophysiologic mechanism of CHI is unclear, but it appears to be immunologically driven. The aim of this study was to obtain a better understanding of the phenotype of the cellular infiltrate in CHI.

Method: We used imaging mass cytometry to achieve in-depth visualization of the intervillous maternal immune cells and investigated their spatial orientation in situ in relation to the fetal syncytiotrophoblast.

Results: We found three phenotypically distinct $CD68^+$HLA-DR^+CD38^+ cell clusters that were unique for CHI. Additionally, syncytiotrophoblast cells in the vicinity of these $CD68^+$HLA-DR^+CD38^+ cells showed decreased expression of the immunosuppressive enzyme CD39.

Discussion: The current results provide novel insight into the phenotype of $CD68^+$ cells in CHI. The identification of unique $CD68^+$ cell clusters will allow more detailed analysis of their function and could result in novel therapeutic targets for CHI.

1. Introduction

Pregnancy is a semi-allogeneic state where the paternally inherited antigens of the fetus are tolerated by the maternal immune system. When the maternal immune system fails to achieve immunological tolerance to fetal antigens pregnancy complications may occur, which could be the case in Chronic histiocytic intervillositis (CHI). CHI is a rare histopathological finding in the placenta. CHI is defined by maternal $CD68^+$ cell infiltrate occupying at least 5% of the intervillous space, in the absence of clinical and histopathological signs of infection [1]. CHI can occur in any trimester and is associated with miscarriage, intrauterine fetal death (IUFD), fetal growth restriction (FGR), and preterm birth [2–5]. The severity of the infiltrate in CHI is correlated with adverse outcome [6–8]. Furthermore, the chance of recurrence in subsequent pregnancies is variable and estimated between 25% and 100% [5,8–10].

The pathophysiologic mechanism of CHI is unclear and current data is often based on small data sets due to the rarity of CHI. CHI appears to be immunologically driven as maternal $CD68^+$ cells, C4d deposition [11] and FoxP3+ regulatory T cells (Tregs) are present [8] in placentas with CHI. High levels of complement-fixing fetus-specific HLA antibodies could be a pathophysiological basis for CHI as has been shown by Benachi et al. [12]. However, not all women with CHI develop fetus-specific HLA antibodies [7]. Reus et al. showed that women with CHI have increased paternal-specific cytotoxic T-lymphocyte precursor frequencies compared to controls with uncomplicated pregnancies [7]. Furthermore, CHI is associated with auto-immune and allo-immune diseases including antiphospholipid syndrome, systemic lupus

* Corresponding author.
E-mail address: m.eikmans@lumc.nl (M. Eikmans).
[1] These authors share last authorship.

https://doi.org/10.1016/j.placenta.2023.05.007
Received 19 February 2023; Received in revised form 15 April 2023; Accepted 13 May 2023
Available online 24 May 2023

erythematosus, and fetal-neonatal alloimmune thrombocytopenia [10,13,14].

Fetal syncytiotrophoblast (SCT) cells are damaged in CHI placentas: they express less CD200 and CD39 [6,15] and more Intercellular Adhesion Molecule-1 (ICAM) [16] compared to unaffected placentas. These molecules are involved in immune cell recruitment and activation of myeloid cells [6,16,17]. Even though myeloid cell numbers are relatively high in CHI, their role and function are not clear and in-depth phenotypic data are lacking. These $CD68^+$ cells have been reported to resemble M2-polarized macrophages [18]. They seem to express CD163 and the complement receptor 4 (CR4; CD11c/CD18), and to not express CD206 and CD209 which are important for endocytosis of pathogens and glycoproteins [18].

In a previous report we identified three dizygotic twin pregnancies with discordant CHI: each pregnancy had one affected and one unaffected twin [19]. These twins create a unique opportunity to study cases and controls exposed to the same maternal immune environment. In this study we enrolled these twin cases for in-depth phenotyping of the $CD68^+$ cell compartment by imaging mass cytometry (IMC) in CHI. IMC allows for the measurement of 40 proteins simultaneously in situ. Furthermore, the spatial orientation of the immune cells was studied in the context of the SCT. This unprecedently detailed characterization of the intervillous infiltrate in CHI is the first step needed to uncover new therapeutic targets and prevent recurrence.

2. Methods

2.1. Patient selection

CHI was diagnosed and scored according to the diagnostic criteria proposed by Bos et al.; at least 5% of the intervillous space was occupied by an immune infiltrate, of which at least 80% were $CD68^+$ cells, in the absence of clinical or histopathological signs of infection [1]. When CHI, villitis of unknown etiology (VUE), or perivillous fibrin deposition was present, it was graded to mild, moderate, and severe/massive based on Benirschke et al. [20].

2.1.1. Samples used for imaging mass cytometry studies

Three dizygotic twin cases were selected from the pathology department at the University Medical Center Utrecht between 2000 and 2015 [19] with UMCU biobank committee approval (TC-BIO number: 16–434) (Table 1). In two cases, one twin was affected by CHI (CHI twin), whereas his or her sibling was unaffected (control twin). Case 3 was a dizygotic twin pregnancy, but the unaffected placenta was excluded, as it did not fulfill the morphologic criteria of a healthy control. In this excluded placenta there were more $CD68^+$ cells present than in healthy control, but less than 5% of the intervillous space was occupied, and therefore did not fit CHI criteria.

2.1.2. Validation cohort

All eleven CHI placentas available in our center and eight healthy term control placentas were included as a validation cohort for IMC results. Samples were selected from the pathology department at the Leiden University Medical Center between 2001 and 2022 (Table 2, Supplementary Table 1). CHI cases that were included were 3rd trimester (9/11) or late 2nd trimester (2/11) to enable comparison to healthy control placenta. This study was carried out in accordance with good practice code, the Declaration of Helsinki and was approved by the Medical Ethical Review Committee Leiden, Den Haag, Delft (study number: B21.034).

2.2. Imaging mass cytometry

2.2.1. Mass cytometry antibodies

IMC antibodies are listed in Supplementary Table 2. Most antibodies were conjugated with heavy metal isotopes in-house using the MaxPar X8 Polymere Antibody Labeling Kit according to the manufacturer's protocol (Fluidigm, California, USA). For five antibodies/isotopes a different protocol was used (Supplementary Table 2). All antibodies were titrated to determine the optimal labelling concentration. Additionally, all antibodies before and after conjugation to a metal were tested by immunohistochemistry before being used in IMC.

2.2.2. Imaging mass cytometry staining

IMC antibody staining was performed as previously described by IJsselsteijn et al. [21]. In short, 4-μm FFPE slides were deparaffinized, antigen retrieval with citrate was performed and the sections were blocked with superblock solution. Next, slides were stained with anti-CD4 (mouse-IgG1, dilution in Supplementary Table 3) overnight at 4 °C. The next day the slides were stained with the secondary anti-mouse-145Gd antibody for 1 h at room temperature (RT). Then the slides were stained with the first mix of metal-labeled antibodies for 5 h at RT (Supplementary Table 3). Slides were washed and stained with the second mix of metal-labeled antibodies overnight at 4 °C. Finally, the slides were stained with Iridium nuclear staining and dried.

2.2.3. Imaging mass cytometry data acquisition

Using a three-element tuning slide the Hyperion was autotuned according to the manufacturer's protocol (Fluidigm). Depending on the size of the intervillous space, 6 to 9 regions of interest (ROIs) from 1 mm^2 of villous tissue were randomly selected and ablated at 200 Hz. ROIs were equally placed 2/3 (CHI/control) subchorial, 2/3 (CHI/control) central and 2/3 (CHI/control) basal.

2.2.4. Data analysis

2.2.4.1. Creating a single cell mask using cell segmentation. Intervillous cells were manually selected for every ROI (Supplementary Fig. 1). DNA staining was used to identify cells, CD141 to identify the SCT lining and consecutive hematoxylin-eosin (HE) staining was used for morphological guidance. After selecting the intervillous immune cells, Ilastik

Table 1
Patient characteristics of twin cases.

Case	1		2		3
Maternal age	24		38		31
Gravidity/ Parity	1/0		1/0		3/2
Gestational age (weeks + days)	34 + 4		39 + 4		37 + 2
Birthweight/ percentile	1380g/p < 3	2750g/ p50-90	3100g/ p10-50	3390g/ p50-90	1460g/p < 3
chronic histiocytic intervillositis	Moderate	Absent	Moderate	Absent	Moderate
villitis of unknown etiology	Absent	Absent	Severe	Moderate	Moderate
Perivillous fibrin depositions	Absent	Absent	Moderate	Absent	Absent

Table 2
Patient characteristics of validation cohort and controls.

	CHI (n = 11)	Control (n = 8)
Median (range) maternal age	34 (20–37)	34 (25–40)
Median (range) gravidity	3 (1–6)	2 (1–3)
Median (range) parity	1 (0–4)	1 (0–2)
Median (range) gestational age (weeks + days)	32 + 3 (23 + 3–39 + 1)	40 + 1 (38 + 4–41 + 2)
Median (range) birthweight percentile	<p3 (<p3 – p10)	P50 (p50 – p90)

(v1.3.3) was used to create a probability map on the selected cells. The probability map was loaded in Cellprofiler (v2.3.1) and exported as single cell mask per ROI.

2.2.4.2. Background removal and data normalization. Semi-automated thresholding is an important step to correct for markers intensity changes due to sample workup procedures and time of storage, as there is a 15 year difference between the samples. Semi-automated thresholding was performed in Ilastik to separate true signal from noise as described previously [22,23]. For each marker, the algorithm was trained to separate noise (0) from signal (1) which resulted in binary pixel values. Therefore, in downstream analysis the marker intensity per cell indicates the proportion of positive pixels in that cell, rather than the marker intensity. Hereby 1 indicates all pixels in the cell are positive, 0.5 indicates half of the pixels in a cell are positive and 0 indicates none of the pixels in a cell are positive for the selected marker. Rarely all pixels are positive due to membrane or nuclear localization. Therefore, visualization of marker expression was set from 0 to 0.5 (all initially above 0.5 will become values of 0.5).

2.2.4.3. Phenotyping of segmented cells. As previously described [24], masks together with binarized thresholded ROIs were loaded in ImaCytE [25]. Each cell in the mask was combined with its corresponding thresholded pixel intensity file, allowing for FCS file exports with marker expression per cell as relative frequency of positive pixels. These single-cell FCS files were analyzed by tSNE in Cytosplore (v2.3.1). In the first tSNE all 5,735 cells were included and major immune lineages were determined. Non-immune cells ($CD45^-$, 522 cells) were excluded from analysis, as were duplicates (11 cells); Cells that have multiple markers belonging to different major immune lineages. In the second tSNE all 2, 970 macrophages and monocytes were included. Based on the dendrogram and marker expressions some clusters were merged.

2.3. Immunohistochemistry and immunofluorescence

Consecutive sections of IMC slides were used for HE staining according to a standardized protocol.

2.3.1. Immunofluorescence staining

Triple immunofluorescence (IF) staining was performed, combining mouse-IgG2b anti-human CD68 (AMP41830, Abcam), rabbit-IgG anti-human CD38 (EPR4106, Abcam), and mouse-IgG1 anti-human HLA-DR (TAL1B5, Dako). In short, slides were deparaffinized and antigen retrieval was performed by microwaving for 10 min in 10 mM citrate solution (pH 6.0). Slides were blocked with Superblock (Thermoscientific, 37580) for 20 min after which the primary antibodies were added for incubation overnight at RT. The next day secondary antibodies were added for 1 h at RT. For CD68/CD38/HLA-DR triple staining; goat-anti-mouse IgG2b-AF594 (Invitrogen), goat-anti-rabbit IgG-AF647 (Invitrogen), goat-anti-mouse IgG1-AF488 (Invitrogen). Slides were covered using 4′,6-Diamidino-2-phenylindole (DAPI)-ProLong Gold (Invitrogen, P36941) and a coverslip. After scanning on the slides (Panoramic MIDI2 scanner, Sysmex), the coverslip and mounting medium were washed away. Finally, the same slides were stained with HE stain and scanned again.

2.3.2. CD39 immunohistochemical staining

Slides were deparaffinized and incubated for 20 min in 0.3% H_20_2. Antigen retrieval and blocking were performed as described above. Primary antibodies were added for incubation overnight at RT, after which goat-anti-mouse/rabbit Ig-HRP (DAKO envision) secondary antibody was added for 1 h at RT. Lastly, slides were incubated with 3,3′-Diaminobenzidine (DAB), counterstained with hematoxylin, dehydrated and covered with a cover slip using mounting medium. Isotype controls were used to confirm that there was no non-specific background staining. Isotype controls were included for all immunohistochemistry (IHC) and immunofluorescence (IF) stains.

2.4. Semi-quantitative scoring of CD39

Since SCT consists of fused cells we could not quantify the number of SCTs expressing or not expressing CD39 and therefore choose for semi-quantitative scoring of CD39 expression on SCT. CD39 expression was scored by three authors (CK, HK and JK; level of agreement 82%). Triple immunofluorescence staining with CD68, CD38, and HLA-DR, together with the HE staining, identified the location of the $CD68^+$ cell infiltrate (affected and unaffected areas) in CHI cases. From unaffected and affected areas a screenshot of three regions per placenta was taken and CD39 expression on SCT cells was scored on a scale from 0 to 2 (0: absent, 1: dim, and 2: bright expression) (scores 0 and 2 represented in Fig. 4C). Scores of three regions from three researchers were averaged. Unaffected vs. affected areas were compared using the Wilcoxon matched-pairs signed-rank test, whereas comparison of unaffected areas from CHI placentas vs. healthy controls was performed using the Mann-Whitney *U* test.

3. Results

3.1. Major immune lineages in the intervillous space

For exploratory in-depth phenotyping of the intervillous immune cells, we designed and optimized a 40-marker IMC panel (Supplementary Table 2) with a focus on the myeloid cell compartment. The clinical characteristics of the dizygotic twins are described in Table 1 and in more detail in van der Meeren et al. [19].

First, five major immune lineage compartments ($CD45^+$) were visualized within the intervillous space: T cells ($CD3^+$), innate lymphoid cells (ILCs) ($CD3\text{-}CD7^+$), monocytes ($CD68\text{-}CD14^+$), macrophages ($CD68^+$), and granulocytes ($CD15^+$) (Fig. 1). Raw marker expression of major immune lineages in the intervillous space is visualized in Fig. 1A and B, where the villi are marked with green dotted lines. We selected the intervillous cells to make a single cell mask after which marker expression per cell was extracted to obtain single cell data (Supplementary Fig. 1). This allowed all intervillous cells and their marker expression to be visualized simultaneously in a single tSNE, and their numbers and frequencies to be determined (Fig. 1C).

We identified 5,202 immune cells (146–2586 per sample). The placenta of the unaffected twin controls had a lower number of immune cells per mm^2 than their CHI twin counterparts (control twins: 46.5 and 19.3, vs CHI twins: 265.5 and 91.7). One cluster showed CD45 expression without any lineage markers, and equal distribution within the immune cell compartment (Supplementary Fig. 2), which was excluded from further analysis. As expected, the $CD68^+$ compartment was abundantly present per mm^2 in the CHI twins (control twins: 7.8 and 7.8, vs CHI twins: 195.6, 74.3 and 96.3). T cell numbers were also increased (control twins: 2 and 0.3, vs CHI twins: 12.8, 4.9, and 15.5) (Fig. 1D). Granulocyte numbers per mm^2 were comparable, but their frequency was higher in the control twins compared to the CHI twins (Fig. 1D and E).

3.2. Six phenotypically different immune cell clusters are identified within the macrophage and monocyte compartment

Next, the macrophage and monocyte compartment (excluding granulocytes) were combined for in-depth phenotyping of the myeloid compartment. Using 17 markers, six phenotypically different macrophage/monocyte clusters were identified (Fig. 2A and B). Clusters 1, 2, 4, 5 and 6 were uniquely found in CHI twins, whereas in the control twin samples cluster 3 was also present. Clusters 1, 2, 4, 5 and 6 most resembled macrophages, with positive CD68 expression and low levels of CD14; whereas cluster 3 (CD14 positive and CD68 negative) showed

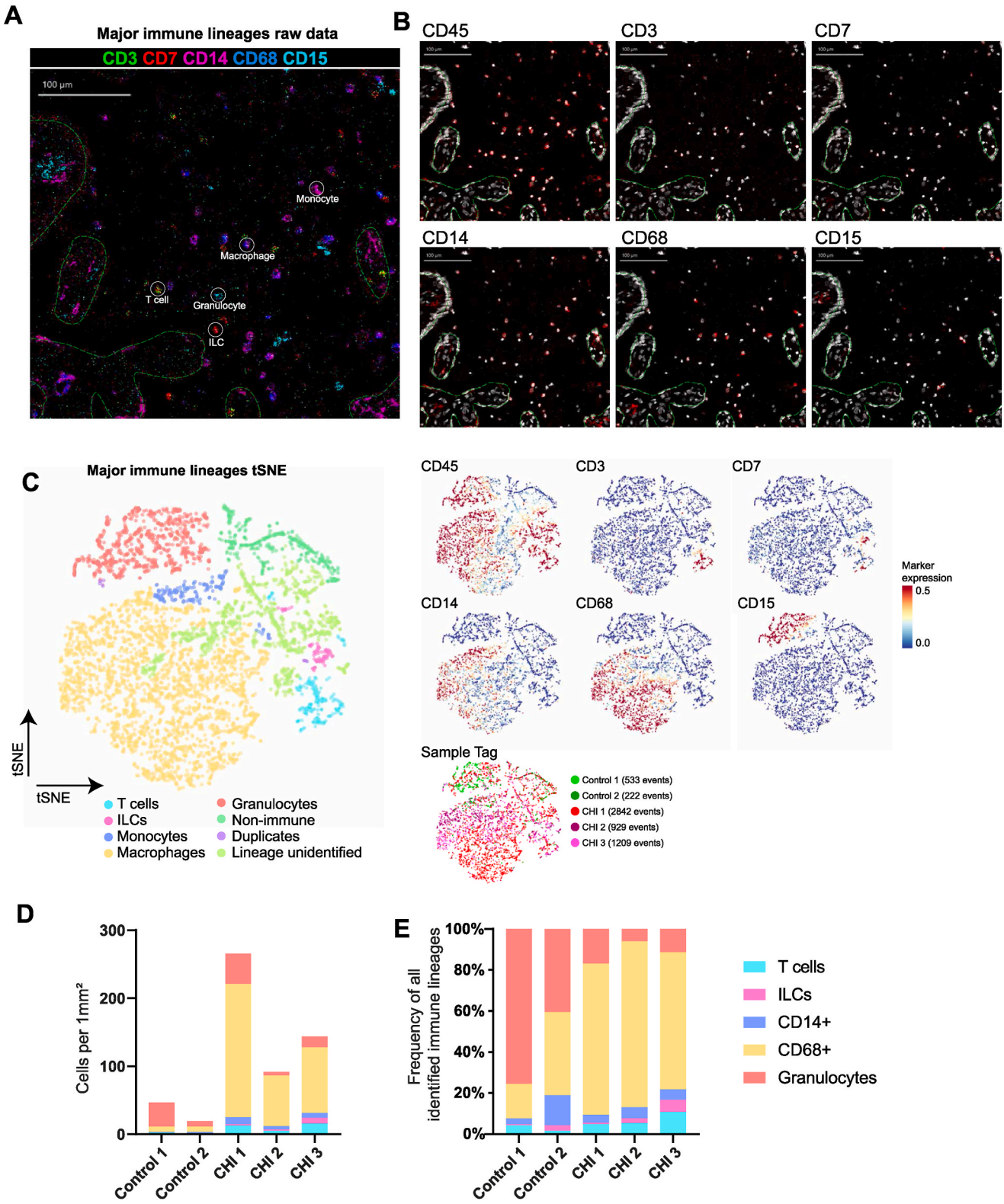

Fig. 1. Major immune lineages in the intervillous space.
Visualization of the major immune lineages in the intervillous space; T cells $CD3^+$, ILCs $CD7^+CD3$-, monocytes $CD14^+CD68$-, macrophages $CD68^+$, granulocytes $CD15^+$. (A) Ex vivo visualization of the major immune lineage markers simultaneously in a CHI twin placenta. Within the green dotted lines are fetal villi, whereas the middle part with the depicted immune cells is the intervillous space. (B) Next, the major immune lineage markers are visualized one by one (red), with DNA staining (white). (C) Single cell phenotyping using tSNE analysis of the intervillous immune cells of the CHI twin placenta and their control twin placentae. Marker expression is visualized from 0 to 0.5, 0.5 indicating that at least 50% of the pixels in the cell are positive for that specific marker. (D) Absolute numbers of the different major immune cell types per 1 mm^2 of tissue slide per sample. (E) Frequency distribution of the different major immune cell types per sample.

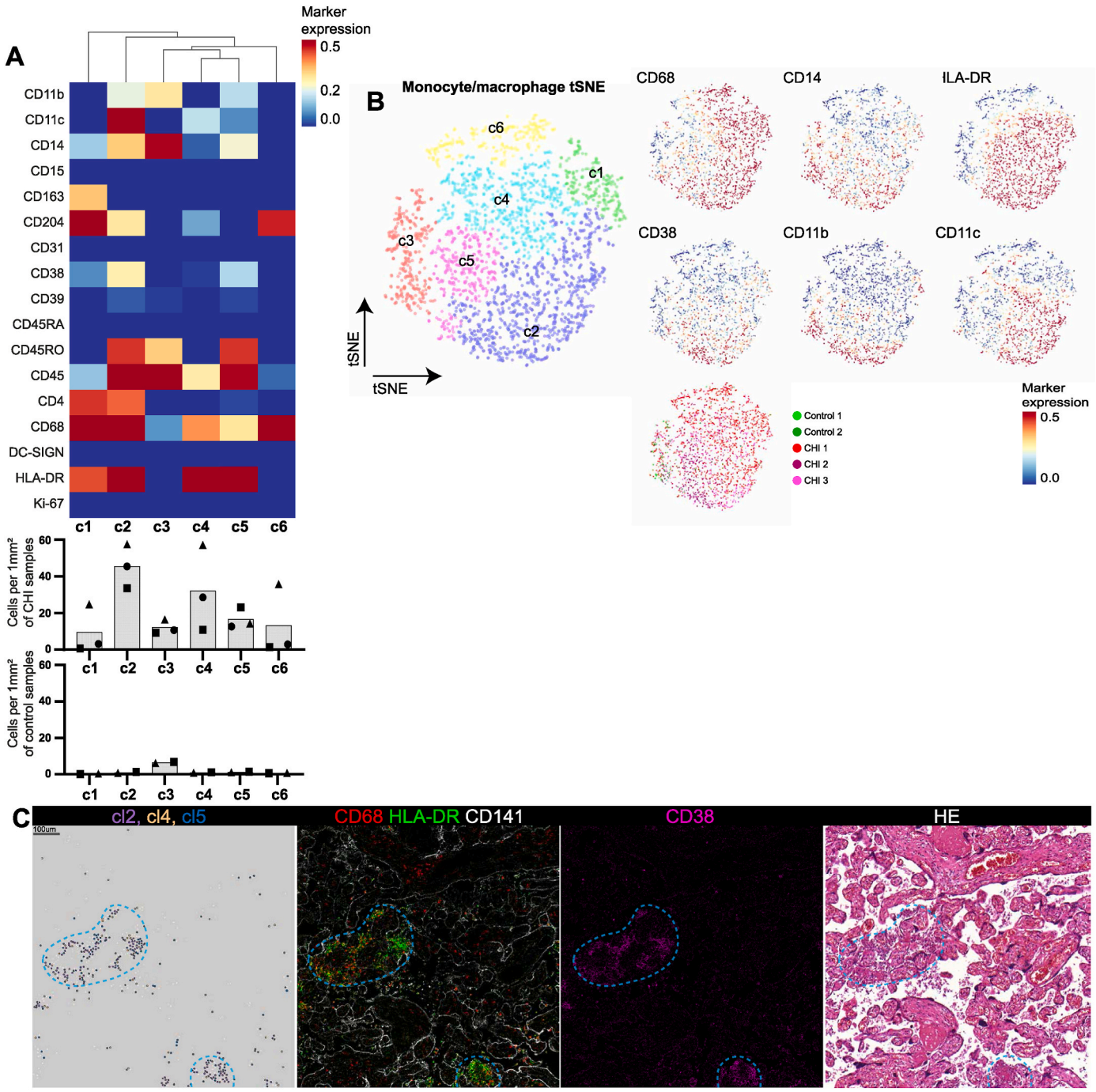

Fig. 2. Phenotypic characterization of the different monocyte/macrophage cell clusters in the intervillous space.
(A + B) tSNE on the monocyte/macrophage clusters using 17 markers. Simultaneous to marker expressions per cluster (A) absolute numbers and means of the 6 clusters per 1 mm^2 of tissue slide is visualized for the CHI twins (upper graph) and the control twins (lower graph). (C) Cluster 2, 4 and 5 plotted back to the tissue location to visualize colocalization (blue dotted lines). Visualizing CD68 (red), HLA-DR (green) and CD38 (light blue) simultaneously (CD141 in white for SCT lining). With a consecutive HE slide.

the greatest phenotypic resemblance to monocytes (Fig. 2A, lower graph).

Clusters 1 and 6 appeared to be sample-specific, since these clusters were mainly present in one CHI twin. Cells in cluster 1 do not express CD11b and CD11c but do express CD163. Cells in cluster 6 expresses CD68 and CD204. Clusters 2, 4 and 5 were observed in the three twins with CHI and absent in controls. Thus, are likely to be CHI specific clusters (Fig. 2A, upper graph). Cluster 2 contains cells with both CD11b and CD11c which also express CD45RO, CD204, CD38, and HLA-DR. Cells in cluster 4 do not express CD11b and CD4, but most cells do express CD11c. Cluster 5 cells also do not express CD4 and CD204. Clusters 2, 4 and 5 have CD11c and HLA-DR expression in common and the three clusters contain cells expressing CD38.

3.3. $CD68^{+}HLA\text{-}DR^{+}CD38^{+}$ cells are present in high numbers in CHI

When visualizing their spatial orientation, cells from clusters 2, 4 and 5 (Fig. 2C) often co-localized with one another. At the specific locations where cells from cluster 2, 4 and 5 colocalize, raw data show that these clusters indeed express HLA-DR (green) and CD38 (light blue), as can

also be observed in the tSNE and heatmap (Fig. 2A).

To confirm our IMC data, immunofluorescence triple staining combining CD68, CD38, and HLA-DR was performed on a validation cohort consisting of 11 placentas with CHI and eight control placentas (Table 2, Supplementary Table 1). We could corroborate the presence of $CD68^{+}HLA\text{-}DR^{+}CD38^{+}$ cells in the intervillous space of all 11 placentas with CHI, with complete absence in controls (Fig. 3).

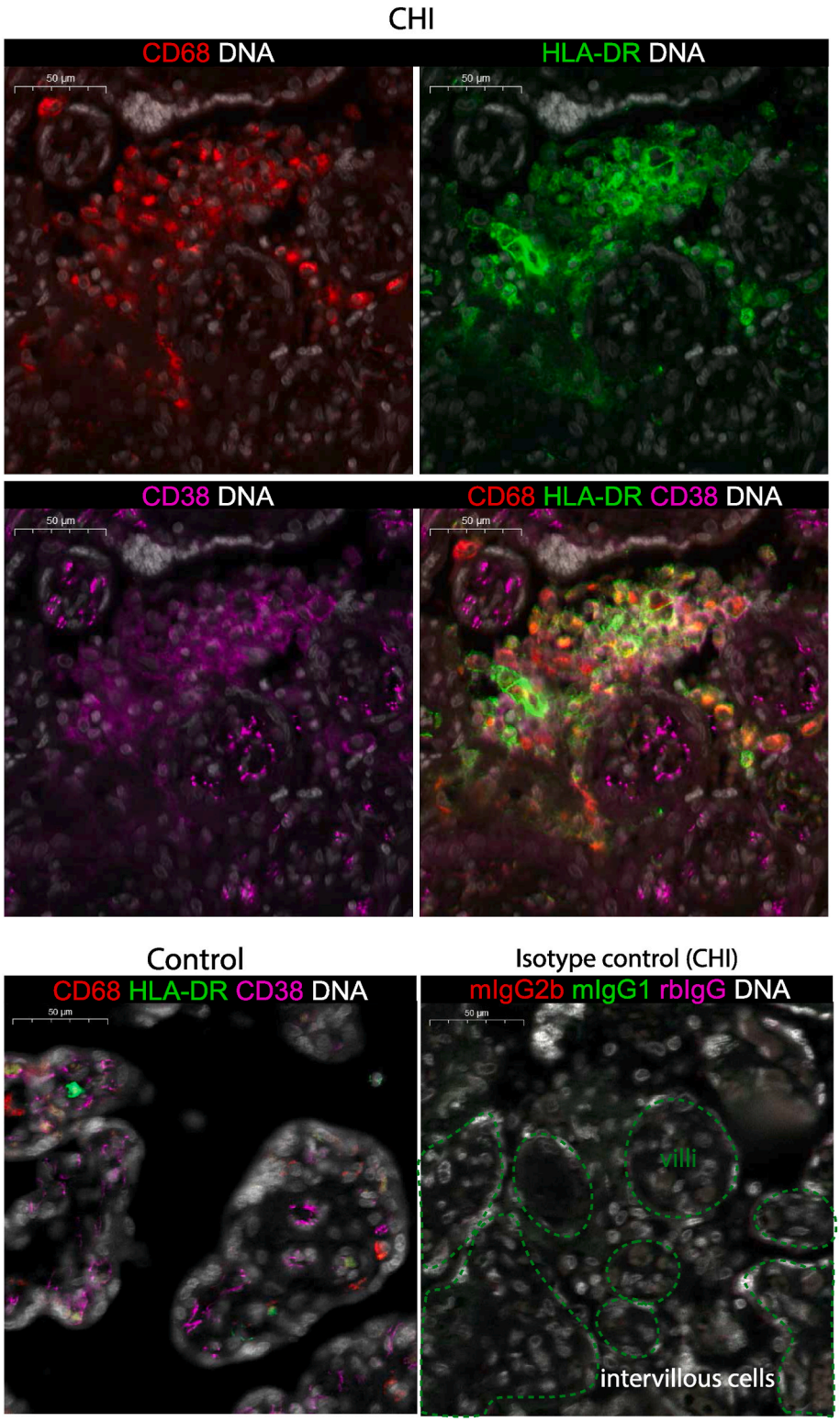

Fig. 3. Immunofluorescence triple staining on validation cohort.
Representative image of the 11 CHI samples that were stained by immunofluorescent staining (CD68 red, HLA-DR green, CD38 light blue, DNA white). Representative image of a healthy control and the isotype control.

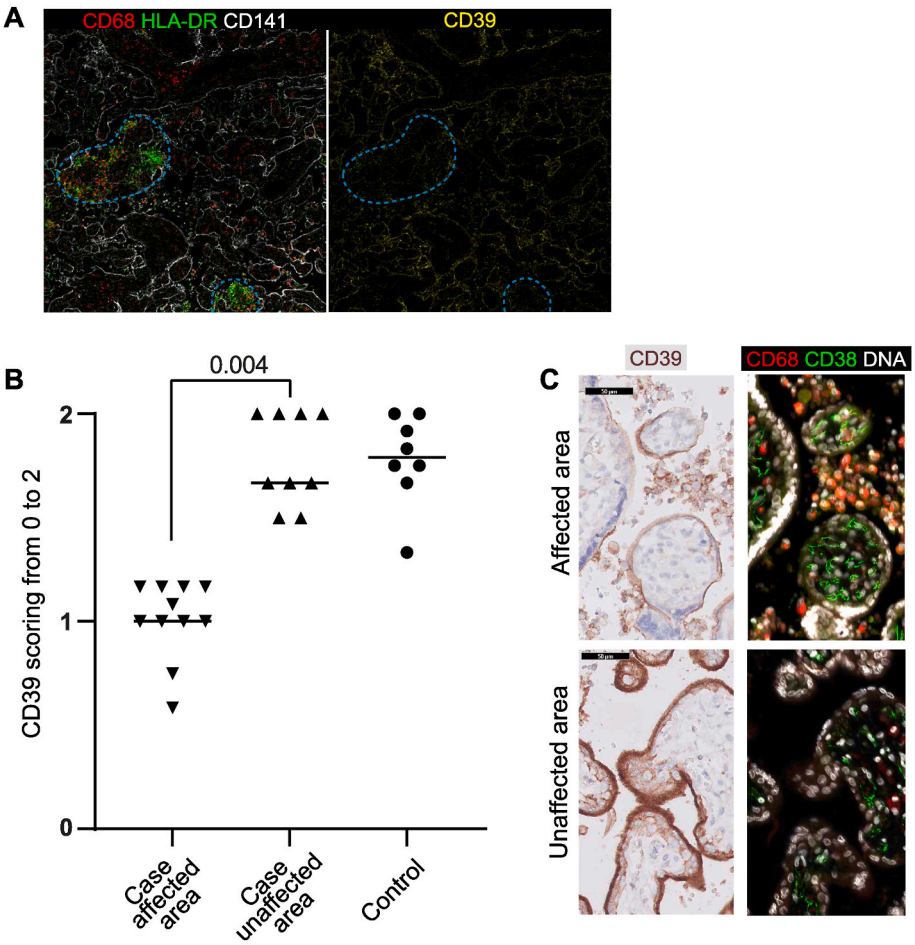

Fig. 4. CD39 expression on SCT.
(A) IMC data showing localization of CD68+HLA-DR+ and CD39 expression. (B) Semi-quantitative scoring of CD39 on SCT cells in CHI placenta validation cohort (Wilcoxon test, median and individual values are shown. (C) Visual representation of CD39 expression in one CHI case are visualized with consecutive slide stained for CD68 and CD38. In the affected area (with $CD68^+CD38^+$ cell accumulation) of this placenta reduced CD39 expression is seen on SCTs compared to the unaffected area (without $CD68^+CD38^+$ cell accumulation).

3.4. Reduced CD39 expression on syncytiotrophoblast cells is specific for regions with CD68+HLA-DR + $CD38^+$ cell infiltrate

Subsequently, we focused on SCT and the localization of $CD68^+$HLA-DR^+CD38^+ cells relative to SCT in CHI vs. control twins. Our IMC panel contains several markers that are expressed by SCT, including PD-L1, CD141 and CD39. No difference was found in the marker expression on SCT between CHI twins and control twins other than in CD39. The immunosuppressive enzyme CD39 has been reported to contribute to maternal-fetal tolerance via the adenosine pathway [26]. In the CHI twins CD39 expression was lower on SCT in regions where $CD68^+$HLA-DR^+CD38^+ cell infiltrates were present (affected areas) compared to areas in the same placenta where these infiltrates were absent (unaffected areas) (Fig. 4A).

Focally reduced CD39 expression was also confirmed in our validation cohort. A lower expression of CD39 on SCT cells was found in affected areas (mean grade: 1) compared to unaffected areas (mean grade: 1.83, $p = 0.004$) of the same sample. The unaffected areas in the CHI cases were graded similarly to control placentas (mean grade: 1.75, $p = 0.88$) (Fig. 4B, Supplementary Fig. 3). Fig. 4C shows a representative image of affected and unaffected areas and the difference in CD39 expression between the two.

4. Discussion

To gain a deeper understanding of the role of intervillous $CD68^+$ cells in chronic histiocytic intervillositis, we applied in-depth immune profiling to tissue sections of CHI placentas and matched (twin) controls using IMC. Five phenotypically distinct $CD68^+$ cell clusters were found in the intervillous space of the CHI twin cases. Clusters 2, 4 and 5 were prominently present and unique for CHI. Cells in these three clusters expressed HLA-DR and CD38 and co-localized with areas where the CD39 expression on SCT was decreased.

The CHI-affected dizygotic twin cases showed a vast increase in placental $CD68^+$ cells, both in absolute numbers and in frequencies compared to their control twin counterpart, which is the defining characteristic of CHI [1]. Besides the major immune lineages, non-immune cells were also found: these cells did not express CD45, nor any other lineage marker of our 40-marker panel. We also found unidentified immune cells expressing CD45 but no other lineage markers. While these cells may be B-cells (no specific B-cell marker was included in the IMC panel), our group previously showed that $CD20^+$ cells are rare in the intervillous space of the placentas of the same twin cases [19]. Alternatively, these cells could be dimly expressing any of the lineage markers. Since the signal in IMC is not amplified by a secondary antibody and the resolution is 1 μm, low marker expression may be missed. The unidentified cells were present at the same frequency for both CHI and control twins, hence we did not characterize them in more detail.

When we specifically focused on the monocyte/macrophage compartment we found three phenotypically distinct clusters unique for CHI. Based on their phenotype these can be designated as macrophage, rather than monocytes. Clusters 2, 4 and 5 are phenotypically distinct from one another by the markers CD204, CD11b, CD45RO and CD4. CD45RO is upregulated in migratory monocytes [27]. CD11c, which all three clusters express, together with CD11b, forms the complement receptors (CR) 3 and 4 in conjunction with CD18. These play a role in phagocytosis, cellular adhesion, and migration within tissues [28]. Ligands for CR3 and CR4 include ICAM, which is found to be upregulated on SCT in CHI [16], and complement factor iC3b, which is likely to be

present during CHI, as C4d deposition and membrane attack complex (MAC) complex formation (C5b-9) have been described on SCT in CHI [11,12]. This suggests that the $CD68^+HLA\text{-}DR^+CD38^+$ cells in the intervillous space may adhere specifically to SCT cells that express ICAM or iC3b. CD204 and CD68 are scavenger receptors, suggesting that cells expressing these markers have the potential to digest damaged/infected cells [29].

All cells of clusters 2, 4 and 5 express HLA-DR and most also express CD38. The CD38 signal is dim and thus could have been missed by IMC. The majority of $CD68^+$ cells in CHI express both HLA-DR and CD38 in the validation cohort. Whereas CD38 can be present on monocytic myeloid-derived suppressor cells [30], in combination with HLA-DR expression it serves as a typical M1 marker [31,32]. Previous literature showed that most intervillous cells express CD163, a typical M2 marker [18]. We found few cells expressing CD163, possibly due to low expression, dim expression can be missed in IMC. It could also be due to the difference in study cohort with Hussein et al., our samples have a higher gestational age compared to Hussein et al. [18]. However, we did observe many cells expressing CD204, a marker also associated with the M2 phenotype. The co-expression of both M1 and M2 markers on $CD68^+$ cells suggests that M1/M2 polarization reflects a diverse spectrum of the myeloid cell population rather than representing a binary cell fate [33].

CD38 expression can be induced in monocytes and macrophages under inflammatory conditions [34], suggesting that the $CD68^+HLA\text{-}DR^+CD38^+$ cells are in an inflammatory state in CHI. In a murine arthritis study, synovial $CD38^+$ macrophages were shown to expand during arthritis. Depletion of $CD38^+$ macrophages by Clodrosome injection or blocking through TNF-α neutralization resulted in alleviated disease [35]. Another autoimmune disease with increased $CD38^+$ mononuclear cells compared to healthy controls is systemic lupus erythematosus (SLE) [34,36]. Interestingly, CD38-targeting treatments are candidates both for rheumatoid arthritis and SLE [37]. However, it should be acknowledged that CD38 is expressed on a variety of macrophages in different types of tissues, limiting its utility as therapeutic target.

Following phenotypic characterization of the $CD68^+$ cell population we investigated whether SCT marker expression was affected in CHI. Our IMC data show that CD39 expression was altered in the CHI twins compared to the control twins. CD39 has been described as an immunosuppressive enzyme in tumor immunology [38]. In CHI pregnancy it previously has been shown that reduced SCT CD39 levels were associated with poor pregnancy outcome [6]. In our study, we found that CD39 expression was decreased in areas with $CD68^+HLA\text{-}DR^+CD38^+$ cell infiltrate but not in unaffected areas of the same CHI placenta. It is not clear if CD39 gets downregulated before the $CD68^+$ cells accumulate in the intervillous space or if this occurs as a consequence of increased numbers of $CD68^+$ cells. Since it is unknown whether CD39 expression changes throughout gestation, as has been described for other markers like PD-L1 [39], we selected relatively high gestational ages for the CHI samples, to optimize the match with the controls. As a consequence of this selection, our CHI group has relatively good pregnancy outcomes (i.e. live birth) compared to other reports [40]. It has previously been described that the severity of infiltrate is associated with pregnancy outcome [41].

Interestingly, CD39 and CD38 come together in the adenosine pathway. Adenosine is an important immune regulatory molecule, as reviewed by Haskó et al. [42]. CD39 and CD38 are ectonucleotidase that are involved in the extracellular production of adenosine. Accordingly, reduced CD39 expression on SCT could result in a microenvironment with less adenosine. However, the presence of cells expressing CD38 could result in the formation of adenosine in the placenta with CHI. We found that both CD203a and CD73, two ectonucleotidases needed to produce adenosine via the CD38 pathway, are also present in the intervillous space of CHI placenta (data not shown). Further studies measuring levels of adenosine in placental blood could elucidate if placenta with CHI have more or less of this immune regulatory molecule.

Furthermore, future studies should focus on the functional capacity of the three macrophage clusters to elucidate their role in CHI. This could eventually result in novel therapeutics such as CD38-targeted treatments. Identification of a CHI-specific cell population could result in the identification of a diagnostic marker for the disease. Since these macrophages are in the intervillous space, it is conceivable that some might be detectable in maternal peripheral blood. Since these cells express scavenger receptors and likely digested placental debris locally, their cargo could potentially be identified as placenta-specific, as has been done previously for a glioma-specific protein [43]. These two characteristics combined could represent a possible detection pathway in which CD38-specific myeloid cells from maternal peripheral blood can be isolated and their cargo can be analyzed, to verify whether they are derived from the placenta. In this retrospective study, peripheral blood samples were not available from women with CHI.

This study is limited in the number of samples used for IMC. This limitation was addressed by confirming results in a validation cohort. Furthermore, since there is a detection limit of dim signals in IMC, corroboration using a different technique is imperative. We therefore used immunofluorescence and immunohistochemistry to confirm our results. Another limitation is that our samples from both the IMC and validation cohorts were of relatively advanced gestational age and therefore associated with disproportionately good pregnancy outcome [40]. However, as explained previously, this was necessary in order to maximize the validity of the comparison with healthy control samples. Therefore, we do not know if this cell cluster is present in early pregnancy losses caused by CHI. Lastly, during patient selection we did not exclude cases with concurrent VUE or perivillous fibrin deposition. Recently it has been hypothesized that CHI cases with or without concurrent VUE and/or perivillous fibrin deposition might have a different etiology. Therefore, we have included the grading of VUE and perivillous fibrin deposition in the patient characteristics tables. Our study cohort includes cases with and without VUE and/or perivillous fibrin deposition and we find the $CD68^+HLA\text{-}DR^+CD38^+$ cells in all the cases.

Currently, there is great interest in the phenotypic characterization and function of the $CD68^+$ cell infiltrate in the intervillous space in CHI, as a similar infiltrate is observed in cases of placental SARS-CoV-2 infection [44,45]. It is not yet clear if the intervillous $CD68^+$ cells in SARS-CoV-2-related CHI are phenotypically and functionally similar to those in idiopathic CHI, where no viral infection is present. Further research could help elucidate this.

In summary, we found three $CD68^+HLA\text{-}DR^+CD38^+$ cell clusters that were distinct for CHI and express receptors that facilitate adherence to the SCT. The identification of these clusters provides an opportunity to study their function in more detail. Furthermore, if detectable in peripheral blood, the $CD68^+HLA\text{-}DR^+CD38^+$ cells could potentially be used as diagnostic biomarkers and may lead to novel therapeutic targets for CHI.

Author statement

J.K. participated in conceptualization of the study, data collection, data analysis and writing the manuscript. L.M. participated in data collection, data analysis and writing the manuscript. M-L.H. participated in conceptualization of the study, data collection, and writing the manuscript. M.I. participated in data collection and data analysis. K.D. participated in data collection and data analysis. H. K. participated in data collection and data analysis. C.K. participated in data collection and data analysis. E.C. participated in writing the manuscript and EC is supported by an MRC Clinical Research Training Fellowship (MR/V028731/1) that funds investigation into the pathogenesis of chronic histiocytic intervillositis. P.N. participated in writing the manuscript. F. K. participated in conceptualization of the study and data analysis. F.C. participated in conceptualization of the study and writing the manuscript. S.H. participated in conceptualization of the study and writing

the manuscript. M.E. participated in conceptualization of the study and writing the manuscript. M.B. participated in conceptualization of the study, data collection, data analysis and writing the manuscript.

Declaration of competing interest

The authors do not have a conflict of interest.

Appendix A. Supplementary data

Supplementary data to this article can be found online at https://doi.org/10.1016/j.placenta.2023.05.007.

References

[1] M. Bos, et al., Towards standardized criteria for diagnosing chronic intervillositis of unknown etiology: a systematic review, Placenta 61 (2018) 80–88.
[2] F. Sauvestre, et al., Chronic intervillositis of unknown etiology: development of a grading and scoring system that is strongly associated with poor perinatal outcomes, Am. J. Surg. Pathol. 44 (10) (2020) 1367–1373.
[3] O. Parant, et al., Chronic intervillositis of unknown etiology (CIUE): relation between placental lesions and perinatal outcome, Eur. J. Obstet. Gynecol. Reprod. Biol. 143 (1) (2009) 9–13.
[4] A. Chen, D.J. Roberts, Placental pathologic lesions with a significant recurrence risk - what not to miss!, APMIS 126 (7) (2018) 589–601.
[5] M. Bos, et al., Clinical outcomes in chronic intervillositis of unknown etiology, Placenta 91 (2020) 19–23.
[6] Y. Sato, et al., CD39 downregulation in chronic intervillositis of unknown etiology, Virchows Arch. 475 (3) (2019) 357–364.
[7] A.D. Reus, et al., An immunological basis for chronic histiocytic intervillositis in recurrent fetal loss, Am. J. Reprod. Immunol. 70 (3) (2013) 230–237.
[8] C. Capuani, et al., Specific infiltration pattern of FOXP3+ regulatory T cells in chronic histiocytic intervillositis of unknown etiology, Placenta 34 (2) (2013) 149–154.
[9] T.K. Boyd, R.W. Redline, Chronic histiocytic intervillositis: a placental lesion associated with recurrent reproductive loss, Hum. Pathol. 31 (11) (2000) 1389–1396.
[10] A. Mekinian, et al., Chronic histiocytic intervillositis: outcome, associated diseases and treatment in a multicenter prospective study, Autoimmunity 48 (1) (2015) 40–45.
[11] R.W. Bendon, et al., Significance of C4d immunostaining in placental chronic intervillositis, Pediatr. Dev. Pathol. 18 (5) (2015) 362–368.
[12] A. Benachi, et al., Chronic histiocytic intervillositis: manifestation of placental alloantibody-mediated rejection, Am. J. Obstet. Gynecol. 225 (6) (2021) 662 e1–e662 e11.
[13] E. Dubruc, et al., Placental histological lesions in fetal and neonatal alloimmune thrombocytopenia: a retrospective cohort study of 21 cases, Placenta 48 (2016) 104–109.
[14] A. Revaux, et al., Antiphospholipid syndrome and other autoimmune diseases associated with chronic intervillositis, Arch. Gynecol. Obstet. 291 (6) (2015) 1229–1236.
[15] D.A. Clark, et al., Changes in expression of the CD200 tolerance-signaling molecule and its receptor (CD200R) by villus trophoblasts during first trimester missed abortion and in chronic histiocytic intervillositis, Am. J. Reprod. Immunol. 78 (1) (2017).
[16] C.A. Labarrere, et al., Intercellular adhesion molecule-1 expression in massive chronic intervillositis: implications for the invasion of maternal cells into fetal tissues, Placenta 35 (5) (2014) 311–317.
[17] N. Koning, et al., Expression of the inhibitory CD200 receptor is associated with alternative macrophage activation, J. Innate Immun. 2 (2) (2010) 195–200.
[18] K. Hussein, et al., Complement receptor-associated CD163(+)/CD18(+)/CD11c(+)/CD206(-)/CD209(-) expression profile in chronic histiocytic intervillositis of the placenta, Placenta 78 (2019) 23–28.
[19] L.E. van der Meeren, et al., One-sided chronic intervillositis of unknown etiology in dizygotic twins: a description of 3 cases, Int. J. Mol. Sci. 22 (9) (2021).
[20] K. Benirschke, S.G. Driscoll, The pathology of the human placenta, in: Placenta, Springer, 1967, pp. 97–571.
[21] M.E. Ijsselsteijn, et al., A 40-marker panel for high dimensional characterization of cancer immune microenvironments by imaging mass cytometry, Front. Immunol. 10 (2019) 2534.
[22] S. Berg, et al., ilastik: interactive machine learning for (bio)image analysis, Nat. Methods 16 (12) (2019) 1226–1232.
[23] M.E. Ijsselsteijn, et al., Semi-automated background removal limits data loss and normalizes imaging mass cytometry data, Cytometry 99 (12) (2021) 1187–1197.
[24] J. Krop, et al., Imaging mass cytometry reveals the prominent role of myeloid cells at the maternal-fetal interface, iScience 25 (7) (2022), 104648.
[25] A. Somarakis, et al., ImaCytE: visual exploration of cellular micro-environments for imaging mass cytometry data, IEEE Trans. Vis. Comput. Graph. 27 (1) (2021) 98–110.
[26] M. Cecati, et al., Contribution of adenosine-producing ectoenzymes to the mechanisms underlying the mitigation of maternal-fetal conflicts, J. Biol. Regul. Homeost. Agents 27 (2) (2013) 519–529.
[27] J. Grisar, et al., Phenotypic characteristics of human monocytes undergoing transendothelial migration, Arthritis Res. 3 (2) (2001) 127–132.
[28] S. Lukacsi, et al., The differential role of CR3 (CD11b/CD18) and CR4 (CD11c/CD18) in the adherence, migration and podosome formation of human macrophages and dendritic cells under inflammatory conditions, PLoS One 15 (5) (2020), e0232432.
[29] J.L. Kelley, et al., Scavenger receptor-A (CD204): a two-edged sword in health and disease, Crit. Rev. Immunol. 34 (3) (2014) 241–261.
[30] T.A. Karakasheva, et al., CD38-Expressing myeloid-derived suppressor cells promote tumor growth in a murine model of esophageal cancer, Cancer Res. 75 (19) (2015) 4074–4085.
[31] W. Li, et al., CD38: a significant regulator of macrophage function, Front. Oncol. 12 (2022), 775649.
[32] K.A. Jablonski, et al., Novel markers to delineate murine M1 and M2 macrophages, PLoS One 10 (12) (2015), e0145342.
[33] M. Nahrendorf, F.K. Swirski, Abandoning M1/M2 for a network model of macrophage function, Circ. Res. 119 (3) (2016) 414–417.
[34] S.A. Amici, et al., CD38 is robustly induced in human macrophages and monocytes in inflammatory conditions, Front. Immunol. 9 (2018) 1593.
[35] D.E. Muench, et al., A pathogenic Th17/CD38(+) macrophage feedback loop drives inflammatory arthritis through TNF-alpha, J. Immunol. 208 (6) (2022) 1315–1328.
[36] M. Burns, et al., Dysregulated CD38 expression on peripheral blood immune cell subsets in SLE, Int. J. Mol. Sci. 22 (5) (2021) 2424.
[37] S. Cole, et al., Integrative analysis reveals CD38 as a therapeutic target for plasma cell-rich pre-disease and established rheumatoid arthritis and systemic lupus erythematosus, Arthritis Res. Ther. 20 (1) (2018) 85.
[38] A. Chow, et al., Clinical implications of T cell exhaustion for cancer immunotherapy, Nat. Rev. Clin. Oncol. 19 (12) (2022) 775–790.
[39] L.M. Holets, J.S. Hunt, M.G. Petroff, Trophoblast CD274 (B7-H1) is differentially expressed across gestation: influence of oxygen concentration, Biol. Reprod. 74 (2) (2006) 352–358.
[40] M. Bos, et al., The severity of chronic histiocytic intervillositis is associated with gestational age and fetal weight, Placenta 131 (2022) 28–35.
[41] C.A. Brady, et al., Immunomodulatory therapy reduces the severity of placental lesions in chronic histiocytic intervillositis, Front. Med. 8 (2021), 753220.
[42] G. Hasko, et al., Adenosine receptors: therapeutic aspects for inflammatory and immune diseases, Nat. Rev. Drug Discov. 7 (9) (2008) 759–770.
[43] W.B.L. van den Bossche, et al., Monocytes carrying GFAP detect glioma, brain metastasis and ischaemic stroke, and predict glioblastoma survival, Brain Commun 3 (1) (2021) fcaa215.
[44] D.A. Schwartz, et al., Chronic histiocytic intervillositis with trophoblast necrosis is a risk factor associated with placental infection from coronavirus disease 2019 (COVID-19) and intrauterine maternal-fetal severe acute respiratory syndrome coronavirus 2 (SARS-CoV-2) transmission in live-born and stillborn infants, Arch. Pathol. Lab Med. 145 (5) (2021) 517–528.
[45] D.A. Schwartz, et al., Placental tissue destruction and insufficiency from COVID-19 causes stillbirth and neonatal death from hypoxic-ischemic injury, Arch. Pathol. Lab Med. 146 (6) (2022) 660–676.